

# Evaluation of Seawater Resistance of a Non-Sintering Inorganic Binder Using Phosphogypsum and Waste Lime as Activators

Kim, Ji-Hoon<sup>1</sup>

Mun, Kyung-Ju<sup>2</sup>

Hyung, Won-Gil<sup>3\*</sup>

*School of Engineering, Muroran Institute of Technology, Muroran, Hokkaido, 050-8585, Japan<sup>1</sup>*

*CMD Group, Wanju-Gun, Jeollabuk-Do, 55338, Korea<sup>2</sup>*

*School of Architectural Engineering, Yeungnam University, Gyeongsan-si, Gyeongsangbuk-do, 38541, Korea<sup>3</sup>*

---

## Abstract

In this study, using Granulated Blast Furnace Slag (GBFS), an industrial byproduct, and Phosphogypsum (PG), and Waste Lime (WL) as activator, non-sintering binder (NSB) which does not require a sintering process was produced, and the chemical penetration resistance was evaluated through a seawater resistance experiment. The result of the experiment showed that the inside of NSB mortar saw almost no influence from the ions in seawater due to its dense structure. Also, as it appears that only the surface reacts with ions in seawater while spreading inward is suppressed, the high seawater resistance of NSB could be confirmed.

---

Keywords : non-sintered binder, seawater resistance, phosphogypsum, waste lime

---

## 1. Introduction

Concrete structures constructed for a marine environment such as floating structures are exposed to the risk of performance degradation such as through rebar corrosion, and as such they must be examined. The performance degradation factors of concrete exposed to a marine environment can be divided into physical factors and chemical factors. Physical factors include marine wave power, wind power, or freeze-thaw; these are caused by the environment. Chemical erosion mostly involves the reaction of cement hydrates with salts such as  $\text{Cl}^-$ ,  $\text{Na}^+$ ,  $\text{SO}_4^{2-}$ ,  $\text{Mg}^+$  which are usually dissolved in seawater, causing the cement hardening body to expand and break and thus degrade[1].

Of these factors, the degradation mechanism involving sulfate is as follows[2,3,4].

- ① The reaction of  $\text{Ca}(\text{OH})_2$ , which is a hydrate product of  $\text{C}_2\text{S}$ ,  $\text{C}_3\text{S}$  and  $\text{MgSO}_4$  in seawater, generates  $\text{Mg}(\text{OH})_2$  and plaster. The generated plaster can be easily dissolved in seawater and thus causes an acceleration of the porosity of the cement hardening body, and a weakening of the structure.
- ② The reaction of  $\text{C}_3\text{AH}_6$ , which is the hydrate product of  $\text{C}_3\text{A}$ , and the plaster generated from the reaction in ① generates ettringite, and the expansion reaction of this ettringite expands and breaks concrete. The use of cement with less  $\text{C}_3\text{A}$  and mixing blast furnace slag granules and pozzolan which reduce  $\text{Ca}(\text{OH})_2$  within the concrete are effective as countermeasures against this.

In the meantime, Friedel's salt is generated as chloride ions in seawater penetrate and react with  $\text{C}_3\text{A}$ , and while a part of it is fixed,  $\text{Ca}(\text{OH})_2$  in cement

---

Received : January 10, 2018

Revision received : February 13, 2018

Accepted : March 5, 2018

\* Corresponding author: Hyung, Won-Gil

[Tel: 82-53-810-2597, E-mail: beda@yu.ac.kr]

©2018 The Korea Institute of Building Construction, All rights reserved.

hydrate reacts to  $MgCl_2$  in seawater to generate  $Mg(OH)_2$  and  $CaCl_2$ , where  $CaCl_2$  is soluble and thus dissolves in seawater, and causes an acceleration of the porosity of the cement hardening body, and a weakening of the structure[5,6].

A typical countermeasure against this is to mix in pozzolan and blast furnace slag granules, which reduce the  $Ca(OH)_2$  in concrete. Such measures densify the internal structure concrete to block the penetration of degradation factors and increase concrete durability.

In the meantime, Non-Sintering Binder (NSB) that is produced based on industrial byproduct Granulated Blast Furnace Slag (GBFS) while using Phosphogypsum (PG), Waste Lime (WL) and the like as activators has been confirmed to have small  $Ca(OH)_2$  generation and form a dense hydration structure[7]. Accordingly, this study intended to produce mortar of Non-Sintering Binder (NSB) and evaluate seawater resistance through artificial seawater soak tests.

## 2. Experiment Overview

The mix of NSB used in this experiment was based on a previous study[8].

### 2.1 Materials

For NSB production in this study, GBFS was taken as the base, PG discharged as waste from phosphoric acid production as a sulfate activator for inducing a hydration reaction, and WL discharged as waste from the Slaked Lime (SL) and  $Na_2CO_3$  production process as the alkali activator. The PG was washed for 5 minutes at  $20^\circ C$  in a 0.5% limewater solution, with the weight ratio of PG in limewater solution 14%. The washed and neutralized PG was transferred to type-II anhydrous gypsum state (II  $CaSO_4$ , APG) calcined at  $450^\circ C$  and to gypsum dihydrate ( $CaSO_4 \cdot 2H_2O$ , DPG) state only dried at  $80^\circ C$ , and was then pulverized and used. For WL, the discharge was dried for 1 day at

$90^\circ C$ , and then was pulverized and used[8,9]. For a comparison of physical properties against NSB, a commercial product was used for Ordinary Portland Cement (hereinafter OPC), and blast-furnace slag cement (hereinafter BSC), in which OPC and GBFS were mixed at 50:50, was produced and used. The physical/chemical properties of material used in this experiment are as shown in Table 1.

Table 1. Chemical properties of raw materials

	SiO <sub>2</sub>	Al <sub>2</sub> O <sub>3</sub>	CaO	Fe <sub>2</sub> O <sub>3</sub>	MgO	Na <sub>2</sub> O	K <sub>2</sub> O	SO <sub>3</sub>	LOI
GBFS	34.8	14.5	41.7	0.5	6.9	0.1	0.4	0.1	0.2
APG	1.3	0.1	41.0	0.04	-	0.1	-	54.9	0.8
DPG	1.1	0.1	32.3	0.2	0.1	-	-	43.3	22.4
SL	-	0.2	65.9	0.1	1.0	-	-	1.1	31.5
WL	4.9	1.6	42.1	1.4	6.9	0.1	1.9	3.1	33.2
OPC	20.9	5.4	64.7	2.4	1.5	0.3	0.2	1.7	2.0

Table 2. Mix proportions of binder (%)

	OPC	GBFS	APG	DPG	SL	WL
BSC	50	50	-	-	-	-
NSB1	-	87	12	-	1	-
NSB2	-	82	-	17	1	-
NSB3	-	81	11	-	-	8

### 2.2 Preparation of Specimens

The mix of NSB is as shown in Table 2. The specimen for measurement of compressive strength and flexural strength for evaluation of seawater resistance was dry-tempered for the materials to mix sufficiently, water (W/B 50%) was added, and then it was mixed with mortar mixer for 1 minute 30 seconds to produce mortar (binder: fine aggregate ratio 1:2.45) in the size of  $4 \times 4 \times 16$  cm. After curing for 1 day in a standard curing room, it was cured for 28 days in water at  $20 \pm 2^\circ C$ . The specimen for microstructure and XRD analysis was dry-tempered so that raw materials measured according to mix conditions could be mixed sufficiently, water (W/C 40%) was added, and then it was mixed with mortar

mixer for 1 minute 30 seconds to produce a paste hardening body, and sealed curing was executed under the curing condition of 20°C, 50%RH up to the anticipated age.

### 2.3 Seawater Resistance

The seawater resistance experiment involved soaking 28-days-old cement mortar in artificial seawater and taking measurements of compressive strength and flexural strength according to KS L 5105. Deterioration Factor was calculated using Equation 1.

Here, DF : deterioration factor (%)

Fw : compressive pressure of mortar soaked in fresh water (MPa)

Fs : compressive pressure of mortar soaked in artificial seawater (MPa)

### 2.4 Hydrate Analysis

To examine the hydration product and microstructure of NSB per age, XRD and SEM analysis was executed. Also, to identify the influence of artificial seawater on NSB hydrate and microstructure, the 5mm-deep part and surface part were taken from the surface of mortar soaked for 1 year and measured.

## 3. Experiment Result and Considerations

### 3.1 Hydration Product XRD Analysis

To examine the hydration products of OPC and NSB binder, XRD analysis was executed according to age, and Figure 1 shows the results. For the OPC, a weak peak of ettringite is observed at the age of the initial 3 days, but not after 7 days. It can be seen that major products are  $\text{Ca}(\text{OH})_2$  and C-S-H gel, and the generation amount has increased with age. In the case of NSB1, it can be seen that there is a large number of crystals of DPG itself at the age of 3 days, while crystals of ettringite appear weak. At the age

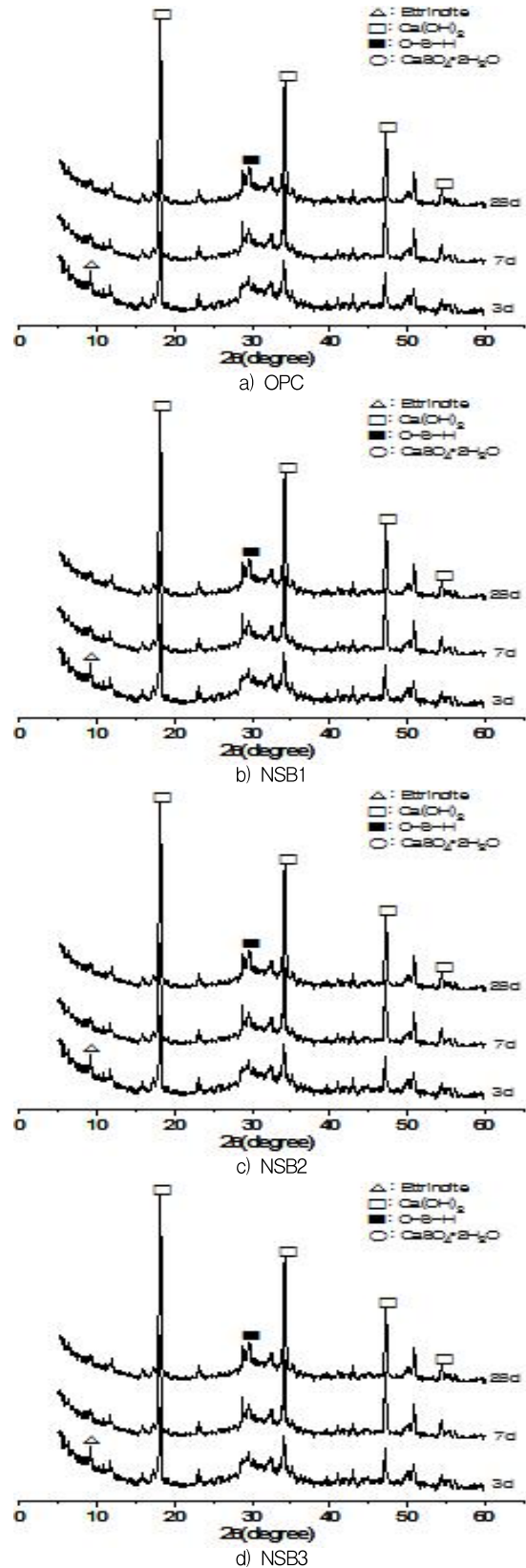


Figure 1. X-ray diffraction patterns of sample with different curing age

of 7 days, major mineral products appear to be ettringite, while the peak of C-S-H (I) gel also shows an increasing tendency compared to at 3 days old, and as time passes, the DPG peak shows a decreasing trend. At the age of 28 days, the major mineral product appears to be C-S-H (I) gel, and the ettringite peak relatively decreases. This indicates that PG which did not initiate a hydration reaction at an early age had remained as minerals itself, and then gradually began to react with GBFS and generate hydrates, and it can be confirmed that the generated ettringite was transferred to the more stable C-S-H (I) gel. Figures 1 c) and d) show the results of XRD analysis according to the age of NSB2 and NSB3 paste using DPG and WL. In the case in which DPG and WL were used, the peak strength of the hydration product at the age of the initial 3 days appeared to be relatively weak compared to the case in which APG was used, but there was no major difference after 7 days of aging. The analysis found that no calcium aluminate hydrate  $C_4AH_{13}$  was generated in the cement paste of any mixes, leading to the judgment that there is no shortage of PG, which is necessary for reaction with GBFS.

In terms of the major mineral products of NSB, hyaline film of GBFS breaks down from alkali stimulation and sulfate stimulation, and the ion eluted from the inside of GBFS reacts with PG to generate ettringite while the remaining components of GBFS gradually form hydrates on C-S-H (I) gel, and at this time, PG is thought to serve not only as an activator, but also as a binder reacting with GBFS [10].

### 3.2 SEM Analysis Result

To observe the degree of hydrate generation according to changes in NSB mix conditions, the result of the SEM analysis is shown in Figures 2~4.

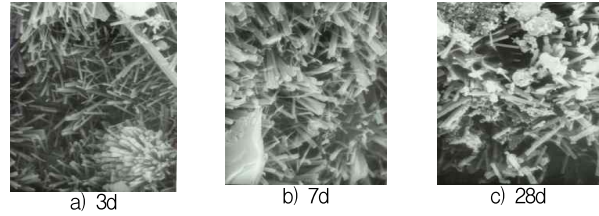


Figure 2. SEM images of NSB1 paste with curing age ( $\times 5,000$ )

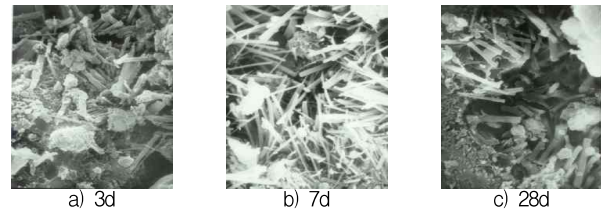


Figure 3. SEM images of NSB2 paste with curing age ( $\times 5,000$ )

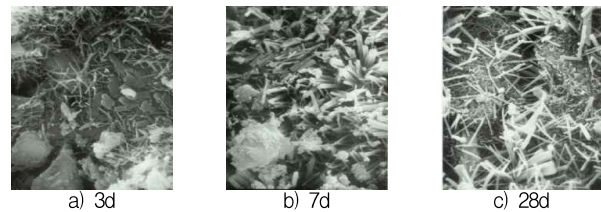


Figure 4. SEM images of NSB3 paste with curing age ( $\times 5,000$ )

Figure 2 shows the internal microstructure according to the age of NSB1 which is mixed with 12% of APG; it can be seen that ettringite at the age of the initial 3 days is generated very densely in a large amount albeit in the form of thin and long needles, and through consistent hydration reaction, it has developed to a thick needle structure form by the age of 7 days. At the age of 28 days, a large amount of tight-form hydrates which appear to be C-S-H gel were observed in addition to ettringite. At the early age, NSB forms strength with tight-form ettringite as the frame, but after a while, ettringite forms a dense network-type web structure with C-S-H gel as the frame, leading to a high expression of strength.

Figures 4 and 5 show the internal microstructure according to the ages of NSB2 and NSB3 which used

DPG and WL. At the age of 3 days, it can be seen that unreacted GBFS and PG exist, around which thin and long needle-shaped ettringite is present. At the age of 7 days, however, it can be seen that a large amount of ettringite is generated, just like in NSB1, and that it has developed to a thick needle form. At the age after 28 days, C-S-H gel is also well developed, the pores of which are observed to be filled up by ettringite.

Combining the result of observing the internal microstructure of NSB paste, the strength expression at early age of hydration is achieved by C-S-H gel generated at the same time, with a large amount of ettringite as the frame. Also, C-S-H gel wraps around ettringite and the amount generated continually increases with age, and the C-S-H gel tightly fills up the pores of the hardened paste, forming a dense network-type web structure with ettringite.

### 3.3 Seawater Resistance

#### 3.3.1 Change in Compressive Strength of Mortar by Artificial Seawater Soaking

Figure 5 shows the changes in compressive strength by period, in which mortar at the age of 28 days of standard curing was soaked in fresh water and artificial seawater.

The compressive strength of mortar soaked in fresh water increased as time passed by, and NSB in particular showed a higher level of strength development compared to OPC.

In the meantime, it can be seen that cement mortar soaked in artificial seawater shows a decrease in compressive strength due to erosion by harmful ions in seawater at 90 days into the soak period. OPC in particular shows a tendency to decrease in strength at 90 days of soaking, and the compressive strength after a 1 year soak period was 37.7MPa, about

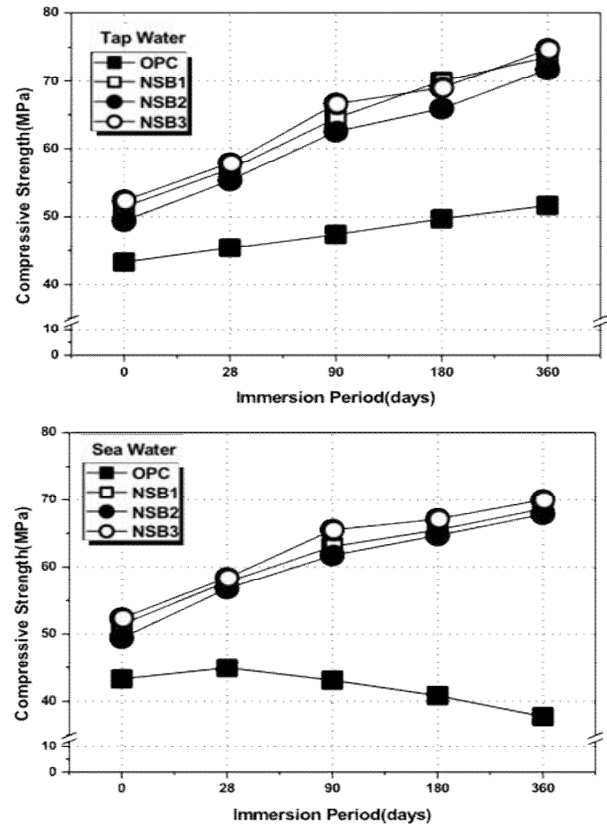


Figure 5. Compressive strength of mortars using various binder with elapsed immersion period in tap water and artificial seawater

15% less than the compressive strength at 28 days of soaking (44.9MPa). This is thought to be because the  $\text{Ca(OH)}_2$  generated by the hydration reaction of  $\text{C}_3\text{S}$  and  $\text{C}_2\text{S}$  among the mineral products of OPC reacts to the  $\text{SO}_4^{2-}$  and  $\text{Mg}^{2+}$  ions in seawater to generate  $\text{CaSO}_4 \cdot 2\text{H}_2\text{O}$  and  $\text{Mg(OH)}_2$ , thus softening the concrete structure. On the other hand, NSB showed a consistent rise in strength during the soak period. This is thought to be because not only is the internal structure sealed to suppress the penetration of harmful ions in seawater, but also no  $\text{Ca(OH)}_2$  is generated during the hydration process, so that it does not react to the  $\text{SO}_4^{2-}$  and  $\text{Mg}^{2+}$  ions in seawater. In addition, NSB2 and NSB3 were almost similar to NSB1, and the compressive strength of NSB1 mortar soaked in artificial seawater for 1 year was found to be 68.7MPa, and 73.6MPa for soaking in fresh water,

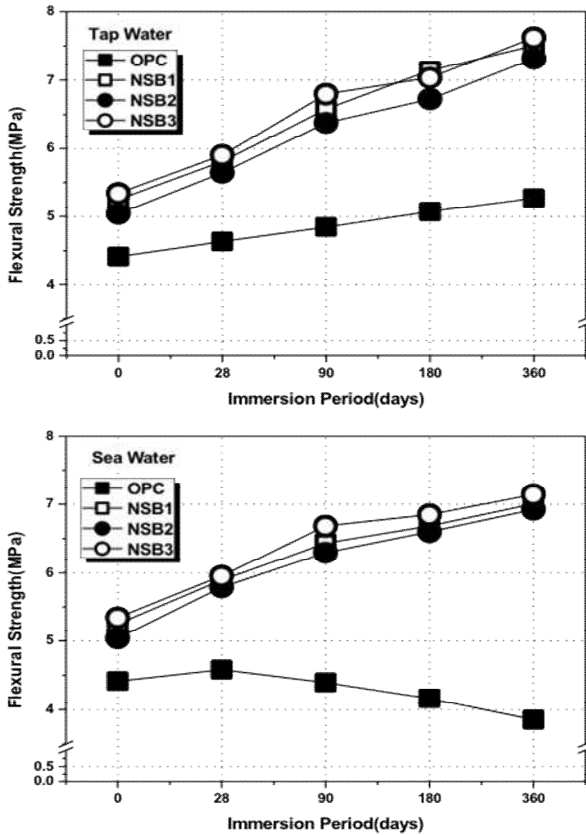


Figure 6. Flexural strength of mortars using various NSBs with elapsed immersion period in tap water and artificial seawater

confirming that there was almost no deterioration caused by artificial seawater.

Figure 6 shows the change in flexural strength by period where mortar was soaked in fresh water and artificial seawater after 28 days of standard curing. Overall, the change appeared to be similar to the change in compressive strength, and NSB mortar exhibited a far greater flexural strength than OPC. It can be seen that the rate of deterioration of the flexural strength cement mortar due to artificial seawater soaking is not as great as for compressive strength.

Figure 7 compares the deterioration factor (DF) of the compressive strength of mortar soaked in artificial seawater with the DF of the compressive strength of mortar soaked in freshwater, and it can be seen that

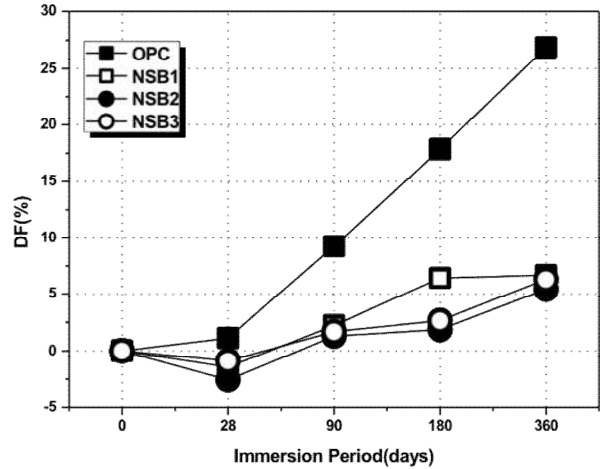


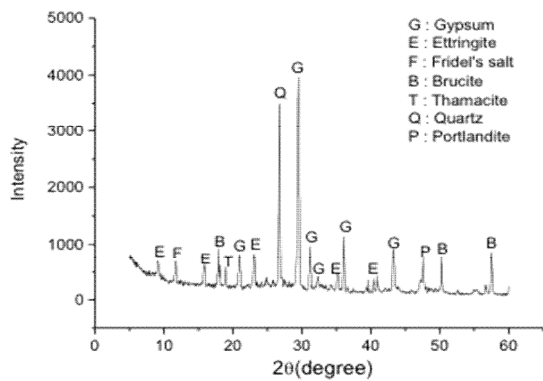
Figure 7. Deterioration factor of cement mortar with type of cement immersed in tap water and artificial sea water

the DF of OPC mortar is greater than that of NSB mortar, regardless of the soak period. On the other hand, in the case of NSB, a reaction product with harmful ions in seawater at an early soak age attached to the surface and blocked the pores of the specimen so that DF up to 28 days of soak period was a negative (–) value, and the DF of OPC mortar for a 1 year soak period was found to be 26.9%, 4~5 times greater than 5.4~6.6% of NSB mortar.

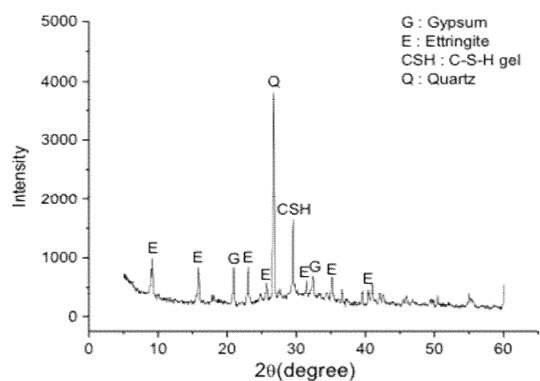
### 3.3.2 XRD and SEM analysis

Figure 8 shows the XRD results of mortar surface soaked for 1 year to examine the influence of artificial seawater on hydration products and microstructure.

The influence of  $\text{SO}_4^{2-}$  ions contained in artificial seawater showed peaks of ettringite and plaster, and it can be seen in particular that the peak of plaster was the strongest. A peak of brucite generated from the reaction of  $\text{Mg}^{2+}$  ions and calcium ions eluted from NSB was also observed. Also, Friedel's salt generated by the penetration of  $\text{Cl}^-$  ions in artificial seawater into the cement hardening body was confirmed, and the peak of thaumasite due to seawater reaction was observed, and portlandite was observed for OPC. Based on the analysis, it is believed that erosion by seawater ions is greater for OPC than for NSB, as



(a) OPC

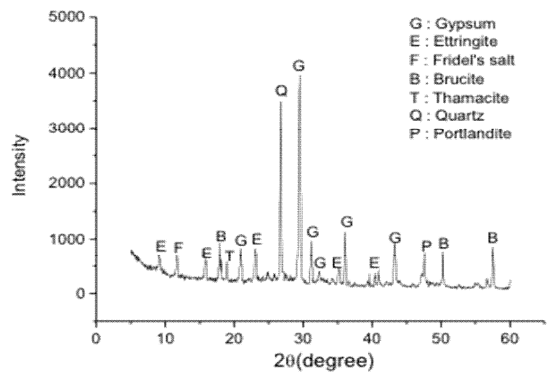


(b) NSB3

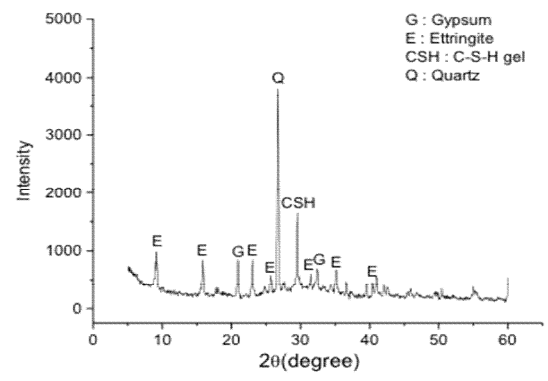
Figure 8. X-ray diffraction patterns of surface of OPC (a) and NSB3(b) mortar after 1-year artificial sea water immersion

the peaks of plaster, brucite and thaumasite appear to be stronger.

Figure 9 shows the result of an XRD analysis of a specimen taken at 5mm depth inside the surface of mortar soaked for 1 year. OPC mortar saw only a slight decrease in peak strength compared to the surface and the strengths were almost identical, showing that the inside of the specimen was influenced by the ions in seawater. Moreover, portlandite peak strength was observed to be larger than at the surface so that deterioration due to reaction with harmful ions in seawater is expected to be more severe during the following period. On the other hand, NSB mortar was found to have seen



(a) OPC

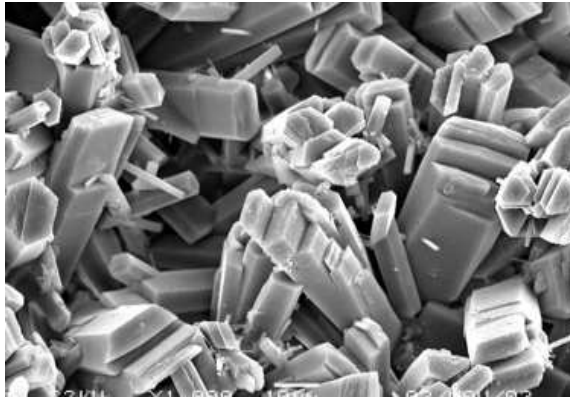


(b) NSB3

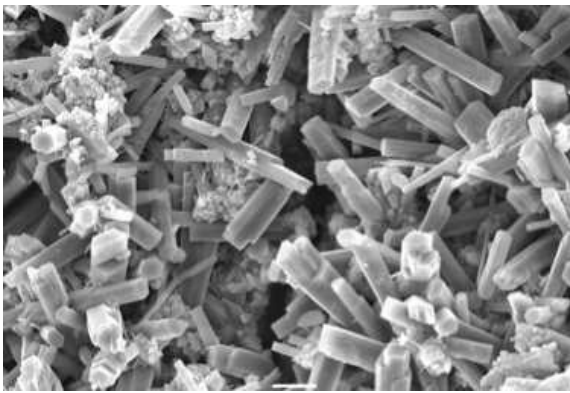
Figure 9. X-ray diffraction patterns of inner 5mm of OPC (a) and NSB3(b) mortar after 1-year artificial seawater immersion

almost no influence from ions in artificial seawater, and major hydrates of NSB such as ettringite and C-S-H (I) gel showed strong peaks. Plaster found in the XRD analysis of NSB mortar is thought to be unreacted DPG contained in NSB rather than  $SO_4^{2-}$  by artificial seawater. Therefore, it is thought that NSB mortar has a reaction to ions in seawater only at the surface and spreading inward has been suppressed, thus having an outstanding seawater resistance.

Figure 10 is the result of an SEM analysis of mortar surface soaked for 1 year. Plaster crystals were clearly observed on both sides, but the crystal sizes differed greatly. Despite having the same soak period and rate for analysis, plaster crystals were further developed for OPC than for NSB, which leads to the judgment that OPC mortar has greater erosion due to the  $SO_4^{2-}$  ions contained in artificial seawater.



(a) OPC



(b) NSB3

Figure 10. Microstructure of surface of mortars with OPC and NSB3 after 1-year artificial seawater immersion

#### 4. Conclusions

In this study, the chemical penetration resistance was evaluated through a seawater resistance experiment of NSB produced using industrial byproducts, and the following conclusion was obtained.

- 1) In terms of major mineral products of NSB, hyaline film of GBFS breaks down from alkali stimulation and sulfate stimulation, and the ion eluted from the inside of GBFS reacts with PG to generate ettringite and the remaining components of GBFS gradually form hydrates on C–S–H (I) gel; at this time, PG is thought to serve as not only an activator, but also as a binder reacting with GBFS.
- 2) By observing the internal microstructure of NSB

binder paste, it was found that the strength expression at early age according to hydration reaction is achieved by C–S–H gel generated at the same time as ettringite, which serves as the frame. C–S–H gel wraps around ettringite, and as the age increases, the amount generated continually increases while C–S–H gel tightly fills up the pores of hardened paste, confirming that a dense network-like web formation is formed with ettringite.

- 3) OPC mortar decreased in strength as the period of artificial seawater soaking increased, while NSB mortar continuously increased in strength. This is thought to be because the internal structure is dense, suppressing the penetration of harmful ions in seawater. As well, no  $\text{Ca}(\text{OH})_2$  is generated during the hydration process, which means that it does not react with the  $\text{SO}_4^{2-}$  and  $\text{Mg}^{2+}$  ions in seawater.
- 4) The reduction in the performance of OPC mortar soaked in artificial seawater was 26.9% for 1 year, which was about 4~5 times higher than the 5.4~6.6% performance reduction seen in NSB mortar.
- 5) Based on the XRD and SEM analysis, the influence of the  $\text{SO}_4^{2-}$ ,  $\text{Mg}^{2+}$ ,  $\text{Cl}^-$  ions contained in artificial seawater led to the observation of ettringite, plaster, brucite, thaumasite, and Friedel's salt. Compared to NSB, OPC had a stronger peak intensity for plaster, brucite and thaumasite, as well as a better development of crystallization, which leads to the judgment that it is subject to a greater influence from seawater ions.
- 6) The inside of OPC mortar was found to be influenced by the ions included in the artificial seawater, but the inside of NSB mortar was found to have received almost no influence from ions in seawater due to its dense internal structure. Also, it is thought that only the surface has reacted with ions in seawater while



---

spreading inward has been suppressed, thus confirming the high seawater resistance of NSB,

slag cement. Architectural Institute of Korea, 2001 Sep;17(9):143–50.

## Acknowledgement

This research was supported by the Basic Science Research Foundation of Korea (NRF), which is funded by the Ministry of Science, ICT and future Planning(No.2015R1A2A2A01005901).

## References

1. Yan PY, Yang WY. The cementitious binder derived with fluorogypsum and low quality of fly ash. *Cement and Concrete Research*. 2000;30(2):275–80.
2. Santhanam M, Cohen D, Olek J. Mechanism of sulfate attack: a fresh look: Part 2, Proposed mechanisms. *Cement and Concrete Research*. 2003 Mar;33(3):341–6.
3. Metha PK, Hu F. Further evidence for expansion of Ettringite by water absorption. *Journal of American Ceramic Society*. 1978 Mar;61(3–4): 179–81.
4. Yimaz AB, Yazici B, Erbil M. The effect of sulphate ion on concrete and reinforced concrete. *Cement and Concrete Research*. 1997 Aug;27(8):1271–9.
5. Torres SM, Sharp JH, Swamy RN, Lynsdale CJ, Huntley SA. Long term durability of portland–limestone cement mortars exposed to magnesium sulfate attack. *Cement and Concrete Composites*. 2003 Dec;25(8):947–54.
6. Ftikos CP, parissakis G. A study on the effect of some Ions Contained in Seawater on Hydrated Cement compounds. *American Concrete Institute*. 1987 Apr;100(1):1651–66.
7. Mun KJ, Hyung WK, Lee CW, So SY, Soh YS. Basic properties of non-sintering cement using phosphogypsum and waste lime as activator. *Construction and Building Materials*. 2007 Jun;21(6):1342–50.
8. Bijen J, Niël E. Supersulphated cement from blastfurnace slag and chemical gypsum available in the Netherlands and neighbouring countries. *Cement Concrete Research*. 1981 May;11(3):307–22.
9. Erdem E, Olmez H. The mechanical properties of supersulphated cement containing phosphogypsum. *Cement and Concrete Research*. 1993 Jan;23(1): 115–21.
10. Park YM, Mun GJ, Soh YS. Effect of Inorganic stimulus agent on compressive strength and pore structure of blast furnace